United Nations Educational, Scientific and Cultural Organization
Land Restoration Training Programme Under the auspices of UNESCO

GRÓ Land Restoration Training Programme
Árleynir 22, 112 Reykjavik, Iceland

Final project 2021

MAPPING RANGELAND DEGRADATION: A THEORETICAL AND PRACTICAL EXERCISE IN THE FOREST STEPPE ZONE, MONGOLIA

Erdenechimeg Avidsuren
Mongolian University of Life Sciences
P.O.BOX 904, Darkhan 45047, Darkhan-Uul
Heychimgee888@gmail.com

Supervisor
Atli Guðjónsson
Soil Conservation Service of Iceland
atli.gudjonsson@landgraedslan.is

ABSTRACT

Rangelands play an important role in providing a variety of ecological services, such as biodiversity preservation, carbon storage, animal forage, and social and cultural value. Rangeland systems are vulnerable and changes can have direct and indirect effects on the environment and the population. However, worldwide, rangelands have been degrading. Effective ways to solve problems related to rangeland management and monitoring include assessing rangelands by using remote sensing. Remote sensing is one methods for evaluating rangeland degradation in an efficient and accurate manner because it can give spatial and temporal information on rangeland management and monitoring on a large scale. The overall goal of this study was to assess the practical usage of remote sensing to identify rangeland degradation in Khongor soum of Darkhan-Uul province, Mongolia. The study attempted to detect rangeland degradation based on NDVI (Normalized Difference Vegetation Index) value. Four classes were identified and mapped, including high-degraded, moderate, low, and non-degraded areas. According to the results, the low degraded class occupied the largest area. The practical aspect of this research was designed to function as a pilot study to gather experience and develop a clearer understanding of the aspects involved in remote sensing of rangeland areas. This may help in future projects to realise the potential and limitations that remote sensing has in this field.

Key words: Rangeland degradation, Landsat, NDVI, Mongolia

This paper should be cited as:

Avidsuren E (2021) Mapping rangeland degradation: A theoretical and practical exercise in the forest steppe zone, Mongolia. GRÓ Land Restoration Programme [final project] https://www.grocentre.is/static/gro/publication/825/document/avidsuren2021.pdf

TABLE OF CONTENTS

LIST OF FIGURES

LIST OF TABLES

ABBREVIATIONS

ALAGAC	Administration of Land Affairs, Geodesy and Cartography
AVHRR	Advanced Very High-Resolution Radiometer
DN	Digital Number
GIS	Geographic Information System
MODIS	Moderate Resolution Imaging Spectroradiometer
NAMEM	National Agency for Meteorology and Environmental Monitoring
NDVI	Normalized Difference Vegetation Index
NIR	Near-Infrared
OA	Overall accuracy
OLI	Operational Land Imager
PA	Producer's accuracy
TIRS	Thermal Infrared Sensor
UA	User's accuracy
RS	Remote Sensing

1. INTRODUCTION

Rangelands provide a variety of ecological services, such as biodiversity preservation, carbon storage, animal forage, and social and cultural value (Archer et al. 2017). However, rangeland degradation has become a global issue with negative consequences for climate and natural habitats. According to Harris (2010) and Mariano et al. (2018), increasing climate change and human activities, as well as land management lacking scientific knowledge and appropriate policies, have had a significant impact on rangeland condition around the world. Assessing rangeland degradation can provide decision-makers with information to help them mitigate the effects of these phenomena.

1.1 Rangeland

Rangeland is defined as uncultivated land that can support both domestic and wild animals (Holechek et al. 2011). Rangeland consists of native plants (climax or natural potential plant communities) such as grasses, forbs, and shrubs (USEPA 2017). In Mongolia rangelands refer to agricultural land with both natural and cultivated vegetation cover for livestock grazing (NSO 2019).

1.2 Rangeland environmental and human roles

Rangeland systems are vulnerable and changes in their condition can have direct and indirect effects on the environment and the population (FAO 2019). Rangeland is a critical resource for the preservation of environmental services such as biodiversity conservation and rural community livelihoods, which is supporting millions of pastoralists, hunters, wildlife, and large numbers of wildlife (ILRI et al. 2021). Rangelands of Mongolia represent approximately 70% of the total national territory and are the mainstay of the rural economy, ensuring food security for the entire country (ILRI et al. 2021). The livelihoods of 200,000 nomadic herder households (NSO 2020) are directly dependent on the rangeland for livestock production in Mongolia. Most of Mongolian inhabitants have direct contact with the land and its benefits.

1.3 Environmental stresses on rangeland

Climate change and related natural phenomena, such as droughts and "*dzuds*", are increasing the risk to Mongolia's economic, social, and human development (MNEGD [Ministry of Nature Environment and Green Development] 2014). The "*dzud*" is a Mongolian term for when large numbers of steppe animals die because of severe icy winter condition. If the winter is too severe, the forage supplies run out, and the animals become weaker, eventually freezing or starving to death. According to a drought and *"dzud"* study, the national drought intensity increased by 2% per year from 1940 to 2010, and the incidence of drought in summer and "*dzud*" in winter increased by 0.6% per year from 1990 to 2010 (Altanbagana et al. 2015). This indicates that the drought and "*dzud*" are intensifying. It is detrimental to pasture yields and food supply, which harms farmers and herders, impacts the population's livelihood and threatens social stability. According to observations from 48 meteorological stations, the average annual surface air temperature in Mongolia increased by 2.07ºC between 1940 to 2014, while air temperature in mountainous areas increased even more (Batjargal et al. 2015). The temperature rises cause soil dryness and flooding which can lead to soil and water erosion. Since 1961, warm seasonal and summer precipitation has been decreasing at a rate of 0.1-2.0 mm/year in Mongolia (MNEGD 2014). Seasonal changes in precipitation affects crop yields, species composition, slow down plant growth, and decrease the number of palatable plants by altering physiological processes,

primary productivity, plant diversity, water table, and increase natural bushfires and invasion of pests (Zhou et al. 2017).

1.4 Human stresses on rangeland

In addition to environmental factors, human activities have a negative impact on rangelands. According to the United Nations (2019), the current global population of 7.7 billion is expected to increase by more than 1.6 billion, reaching 9.3 billion by 2050. As the world's population increases, so does the demand for food production. As the number of livestock increases, pressure on rangeland vegetation significantly increases as well. Rangeland area is limited, and humans have converted large areas of rangeland to cropland, further reducing their coverage. Roads in connection to mining and urbanization also reduce rangeland area and have a negative impact on the rangelands. Due to the many poor roads, the surrounding soil has been severely damaged, and pasture plants degraded, which makes livestock grazing impossible.

1.5 Rangeland degradation

Rangeland degradation is accelerating on a global scale, resulting in a sharp decline in rangeland productivity around the world (GEF 2014). Rangeland degradation is characterized by a decrease in productivity (yield) in some parts of a rangeland ecosystem, species depletion, and negative soil changes. Plant diversity, height, vegetation cover, and plant productivity all suffer because of rangeland degradation (Fenetahun et al. 2018). Rangeland degradation is caused by flooding, soil erosion, overgrazing, livestock husbandry, livestock numbers, structures, pests, rodents, well water supply, fires, agricultural technology, and poor roads in Mongolia (MNEGD 2018). Densambuu et al. (2018) found that 57% of Mongolia's total rangeland was degraded in some way. According to the Jigjsuren et al. (2015) study, which polled 54% of herders, pasture yields have declined in the last 20 years. In that study 61.3% of herders reported the number of palatable plants has decreased, while 37.1% reported an increase in the amount of bare land in pastures. The reason for this was explained as soil deterioration, increased sand movement (39.5%), and soil erosion (50.8%) (Jigjsuren et al. 2015). It is still unclear how to effectively avoid the degradation risks. Thus, it is important to assess the rangeland degradation risk as the first step in predicting the risk of degradation.

1.6 Rangeland monitoring and evaluation

Existing rangeland evaluation strategies are classified into two types: traditional field methodologies based on fieldwork and surface cover measurements, and remote-sensing methodologies characterized by non-observations with restricted fieldwork (Svoray et al. 2013). Remote sensing is the process of detecting and monitoring an area's physical features from a distance by measuring its reflected and emitted radiation. Remote sensing data collection appears to be the most logical approach to obtaining appropriately data and information over large areas in short time periods and at random positions far from easy surface access (Booth & Tueller 2003).

Mongolia currently has two national monitoring programs in place to assess condition of rangelands, which rely on networks managed by the National Agency for Meteorology and Environmental Monitoring (NAMEM) and the Administration of Land Affairs, Geodesy, and Cartography (ALAGAC). At the national level, NAMEM provides long-term trends in vegetation and rangeland condition, whereas ALAGAC assesses the impacts of grazing management at the local level (Densambuu et al. 2018). Nonetheless, by conducting ground surveys, these approaches to rangeland assessment necessitate a significant investment of time,

money, and labour. Rangeland areas are generally large and inaccessible, making ground surveys difficult to determine the condition of the ecosystem. These monitoring systems are intended to assess the current state of the rangeland. However, there are currently very few studies in Mongolia that examine where there is risk of rangeland degradation. Although the current national rangeland monitoring and assessment system should provide accurate data on rangeland condition, there is still a need for a more cost-effective system that meets the higher time and cost-effectiveness criteria. This was the primary motivation for conducting the current study: to conduct a practical exercise using geographic information system (GIS) and remote sensing (RS).

Remote sensing is one method that can be used for evaluating rangeland degradation in an efficient and accurate manner because it can give spatial and temporal information on rangeland management and monitoring on a larger scale. GIS and RS have been widely used for rangeland evaluation, including assessing rangeland and pasture condition (Vanderpost et al. 2011), indicating vegetation deterioration (Karneili et al. 2013), investigating variations in vegetation dynamics (Hilker et al. 2014), and assessing pasture manufacturing capacity (Boschetti et al. 2007).

1.7 Remote sensing approach for rangeland evaluation

The availability of remotely sensed data provided a long-term and large-scale opportunity because it is strengthened by the ability of the data sets to present vegetation and land surface at large spatial and temporal extents (Tong et al. 2019). As a result, remote sensing is a well-known and effective method for assessing rangeland (Matongera et al. 2021). Because of their low cost and constant availability across large and remote areas, time series of remote sensing data are frequently used to estimate the extent and intensity of rangeland degradation (Eddy et al. 2017). The most common satellite data sources include Landsat (Tomaszewska et al. 2020; Nguyen et al. 2020), AVHRR (Advanced Very High-Resolution Radiometer) (Fontana et al. 2008), MODIS (Moderate Resolution Imaging Spectroradiometer) (Cao et al. 2015), Sentinel-2 (Vrieling et al. 2018). However, the applications of each of these data sources present various challenges and opportunities in research. For example, early sensors like AVHRR and MODIS have a high temporal resolution that allows them to detect subtle changes in vegetation development, but they have a low spatial resolution which makes it difficult to detect plant-specific changes (Shen et al. 2015). Medium and high spatial resolution sensors, such as Sentinel-2 and SPOT, with a temporal resolution of 3–10 days, on the other hand, do not provide adequate time series data for characterization of vegetation changes, particularly in areas with constant cloud cover (Misra et al. 2020).

Landsat data is available for free. It is compatible with ArcGIS and widely used. It is also comparatively easy to learn how to use it and a lot of supporting reading material about previous research projects using this data exists. For these reasons it was decided to use Landsat data for this study.

Landsat satellites have sufficient ground resolution and spectral bands to track land use and report land change due to global warming, drought, biomass variations, fires, and a variety of all other natural and human-made changes (USGS 2020). The Landsat-8 imagery used in this study has a moderate resolution (30 m) and can be acquired repeatedly (every 16 days) from the earth's surface. A main aspect of Landsat Collection 2 is the significant improvement in the absolute geolocation accuracy of the worldwide ground reference dataset. It also includes upgraded global digital elevation modelling sources, as well as calibration and validation

updates (USGS 2020). Landsat sensors offer Level-1 data as their standard output (Pinto et al. 2020). Also, level 1 of Landsat-8 data has units of Digital Numbers (DNs) that are easily established to the top of the atmosphere (TOA) reflectance and spectral radiance. Due to these advantages, collection 2 level 1 data were chosen for this study. Landsat 8 satellite data collect values of spectral bands such as Near-Infrared-band 5 (0.85-0.88 μm), RED-band 4 (0.64-0.67 μm), as was the case in this study. Furthermore, the NIR band detects a healthy reflect of vegetation, terrestrial plants and dry soil which are highly reflected. RED band is more widely used for vegetation. Therefore, these two bands were chosen due to rangelands being characterised by both soil and vegetation areas.

The NDVI (Normalized Difference Vegetation Index) is the most widely used index in various rangeland zones around the world (Colombo 2012; Karneili et al. 2013; Ünal et al. 2014). The NDVI is used to identify changes in land cover caused by natural and human activity (Hashim et al. 2019).

The benefits of satellite data include the fact that it is in digital format and is simple to integrate into a geographic information system (GIS). Furthermore, the use of satellite remote sensing data to carry out land and vegetation change is relatively inexpensive when compared to conventional methods which mostly involve physical data collection on the ground for the whole area. Against this background, this case study used remote sensing to detect rangeland degradation in the Khongor soum.

1.8 Overall goal and objectives

The overall goal of this study was to assess the practical use of remote sensing to quantify rangeland degradation in Mongolia forest steppe zone.

The following objectives were developed based on the research goal:

1. To study a remote sensing approach for rangeland evaluation.
2. To evaluate the applicability of this methodology by carrying out a case study on the forest-steppe zone in Mongolia.
3. To identify and map degraded areas.

2. CASE STUDY AREA

2.1 Description of case study area

Mongolia is a landlocked country in Central Asia between Russia and China (Figure 1). It has a total area of 1,564 million square kilometres. Mongolia has a continental climate with major daily and annual temperature fluctuations. Because of the geographical location, mountainous terrain and climate, winters are long and cold with little precipitation, while summers are hot. Nearly 80% of the annual precipitation falls during in the growing season. The precipitation ranges from 50 mm in the desert to more than 300 mm in the Khangai and Khentii mountain regions. Mongolian rangelands account for 70% of the country's total land area (NSO 2019). The Mongolian plateau is divided into six natural zones: mountain, taiga alpine, forest-steppe, steppe, *"gobi"* and desert.

The case study area is Khongor soum of Darkhan-Uul province, which is in the Khentii mountain range (Fig. 1), which is characterized by mountains covered in forest-steppe zone. The forest-

steppe zone is the major area of Mongolian rangelands type, accounting for 25% of Mongolia's total territory (Bayaraa 2019). The study area is in the valley of the Kharaa river, a low hill between the mountains of the Khentii mountain range. The main vegetation forms are mountain steppe and steppe variants shrub, and grass. The case study area contains low-lying slopes, flat plains, and a few rivers. The total territory of Khongor soum is 263,957 ha, with 193,690 livestock (horse, cattle, camel, sheep, and goat) grazing during all four seasons of the year (Fig. 2). Between 2011 and 2020, the number of livestock increased by 71.27% (NSO 2020). One of the causes of this increase was an influx of herders from remote provinces to Darkhan-Uul province to get closer to the market, because Darkhan-Uul province is close to the capital city.

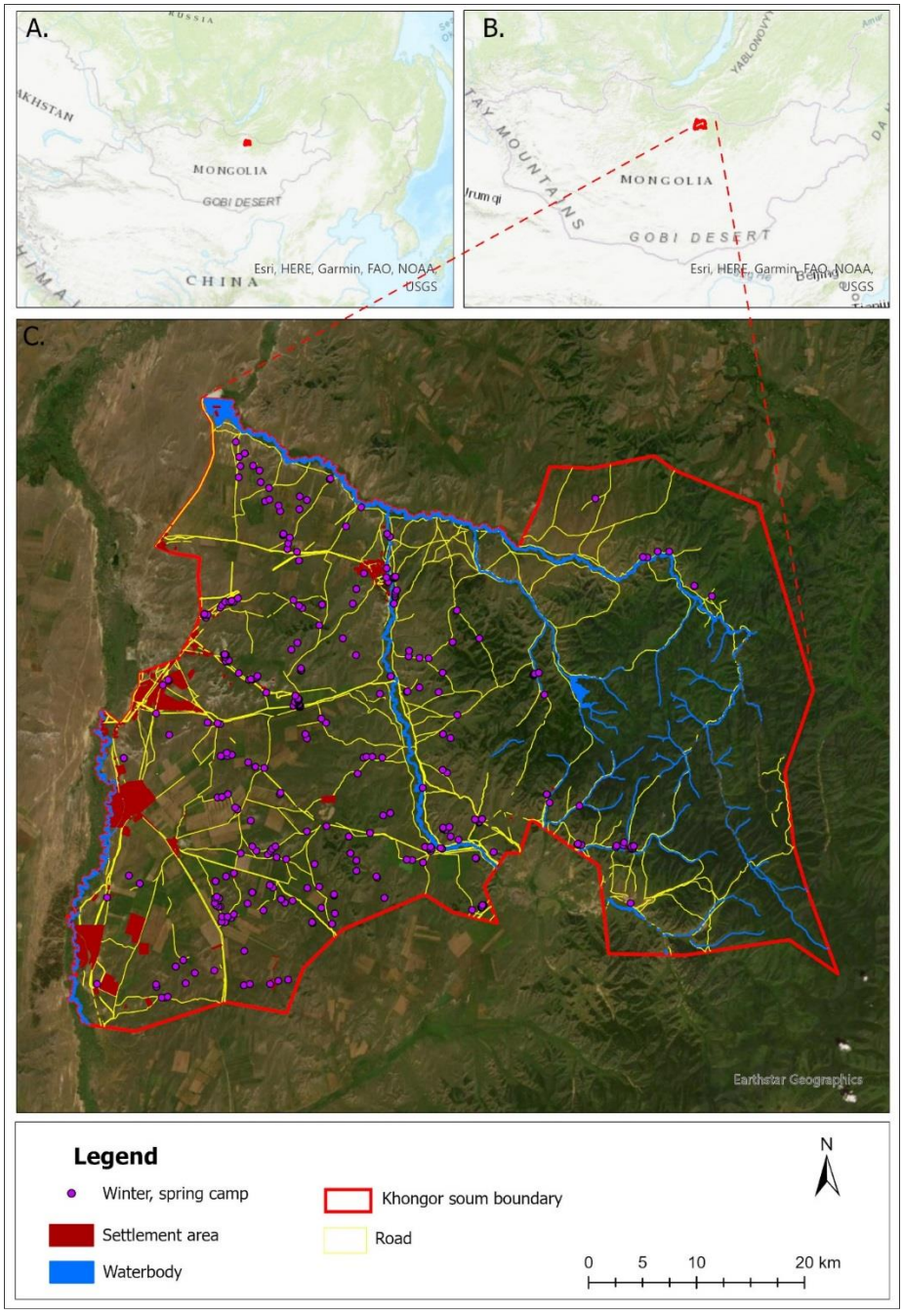

Figure 1. Map of case study area: A. Location of Mongolia on the world map; B. Location of case study area on the map of Mongolia; C. Map of case study area Khongor soum. (USGS 2021).

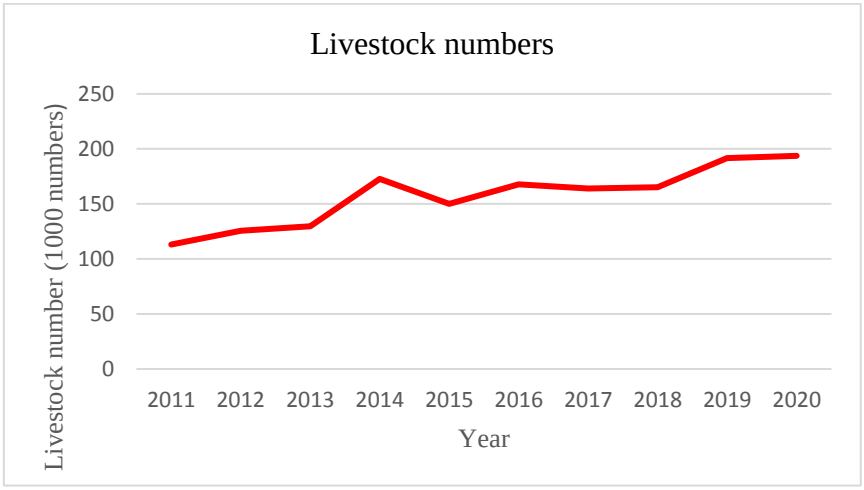

Figure 2. Livestock numbers of Khongor soum in 2011-2020 years. (Source: NSO 2020).

Darkhan-Uul province is a central part of Mongolian agricultural zone, which is in central part of Selenge province in the middle of the Khangai and Khentii mountain regions. Darkhan-Uul province is a significant agricultural area in Mongolia. The Khongor soum is the largest district in Darkhan-Uul province, approximately 230 km northwest of capital city Ulaanbaatar, close to the southern border of Russia.

2.2 Soil

The soil type of Khongor soum includes the Khangai-Khentii region's soil. The dominant soil type of the province is brown soil of the dale steppe in Darkhan, and meadow soil spread over the valley of the River Kharaa (Narmandakh 2009). The mountainous and forested areas are dominated by mountain Histosols. The soil cover is thin and lies on top of a layer of gravel. The Chernozem and Kastanozem soils are found in mountainous areas and areas without forests. The Chernozem is a soil with a high level of fertility. The foothills are dominated by thin Leptic Kastanozem soils. The Gleyic Kastanozem soils are mainly stabilized in the river valleys between the mountains. The Gleyic Kastanozem soils have a high level of fertility and are used for agricultural production.

2.3 Meteorological information

The case study area has a harsh natural climate due to the area's characteristics, patterns, and differences in depressions and convexities, with large differences in the four seasons of the year, high temperature fluctuations, and low precipitation. The wind blows from the north, north-east, and north-west. The annual wind force is calm for 60.8% of the year, but it rises to 10–25 m/s in early March and can reach 28–32 m/s. The case study area has a hot dry summer and cold winter. However, the cold winter can go on for a long time with ground frost. During the summer, the daytime can be very hot, but while cooling at midnight, and the wind speed is higher during the daytime and lowering at night, usually resulting in poor precipitation. These are the features of a harsh continental climate that affect the growth of specific plant species and vegetation. The annual rainfall averages 250-300 mm in the mountain's region, and 150-200 mm in the steppe region. Most of the precipitation falls during the vegetation growing season. The region's summer average temperature ranges between 15-20ºC. According to estimates there is, little change in precipitation in the case study area, the average temperature in the summer months decreased by 1.0-3.0ºC, and in the winter months by 1.4-3.6ºC in the last

decade (IRIMHE 2021). Precipitation and temperature data were obtained from the nearest meteorological station of Darkhan and were acquired from the Mongolian Information and Research Institute of Meteorology, Hydrology and Environment. The annual average temperature is 0.6ºC, with the summer average temperature +17.8ºC (1981-2010 years' average) in June, July, August, and the winter average temperature -19.7ºC (1981-2010 years' average) in December, January, and February (IRIMHE 2021). The daily average temperature +19.6ºC from July 10 to August 19, 2020 (Figure 4). In the study period average temperature was 1.9ºC higher than the average summer temperature, which was a relatively hot period.

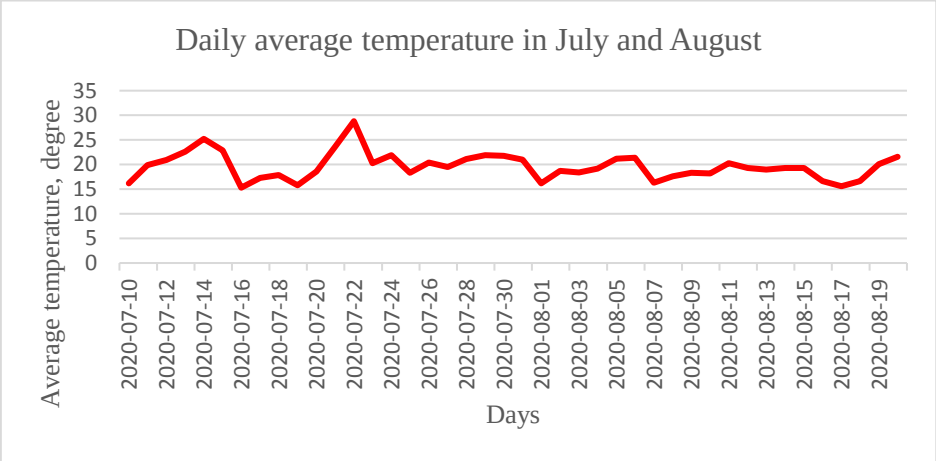

Figure 3. Daily average temperature from July 10 to August 19, 2020. (Source: IRIMHE 2021).

In Mongolia, approximately 85% of the total precipitation falls between April and September, with the majority of precipitation falls in July and August, accounting for 50-60% of total precipitation (Batima et al. 2005). The annual precipitation is 301.2 mm with the highest precipitation 77-86 mm in July and August, and the lowest precipitation 2.8-2.9 mm in February and March. During the study period, from July 10 to August 19, 2020, there was less precipitation, the total precipitation was 107.6 mm, and the study period average precipitation was 2.5 mm (Figure 4). It was lower than the summer average precipitation. The highest rainfall 49 mm was registered on the 1st of August 2020. The temperature and precipitation showed that it was a hot and dry summer.

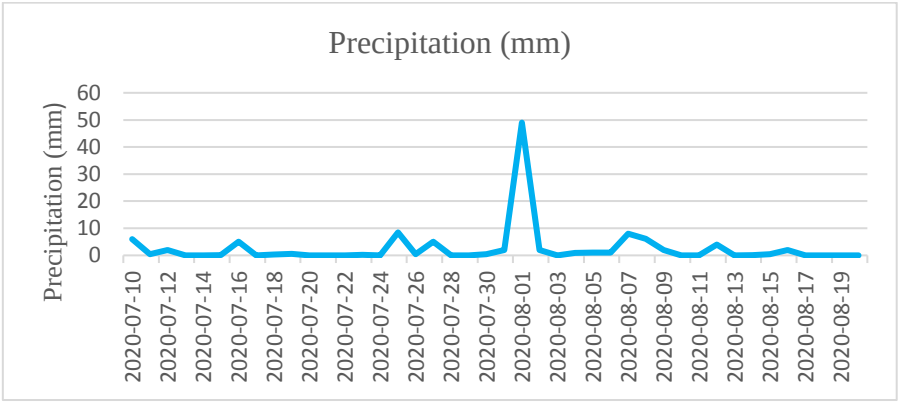

Figure 4. Precipitation from July 10 to August 19, 2020 in case study area. (Source: IRIMHE 2021).

3. THE BASIS OF REMOTE SENSING RESEARCH WORK

3.1 Image pre-processing

Every unprocessed remotely sensed image contains errors. Pre-processing is the process of correcting such errors before the data are used (Shankar et al. 2020). The term derives from the fact that pre-processing is required for proper processing to occur. Pre-processing is commonly considered in the context of digital analysis of remotely sensed data by two forms of data correction (Matongera et al. 2021): (1) radiometric pre-processing, which addresses pixel intensity differences (DN- digital number); (2) geometric correction corrects pixel-relative position errors caused primarily by sensor viewing geometry and terrain variations. Landsat-8 data originate from two sensors; these are the Operational Land Imager (OLI) and the Thermal Infrared Sensor (TIRS). The OLI and TIRS sensors are combined to develop a single product. The single product is radiometrically and geometrically corrected, co-registered with correction and called the Level 1 product (Matongera et al. 2021). In this case study, Landsat 8 data is utilized due to the availability of radiometrically and geometrically corrected data images.

3.2 Image enhancement

The goal of image enhancement is to enhance visual interpretability of an image by increasing the obvious contrast between the features of the scene (Thomas & Ralph 2000). The goal of visualizing digitally enhanced imagery is to maximize the combined abilities of the human mind and the computer. The mind is good at defining spatial attributes on an image and can differentially define unclear or subtle features selectively. The human eyes are incapable of distinguishing subtle spectral or radiometric differences that may characterize such attributes. The goal of computer enhancement is to visually enhance these minor differences so that they can be seen (Thomas & Ralph 2000). Image enhancement examples include removing noise from images, sharpening images, adjusting image intensity, and making object detection easier (Petros 2005).

3.3 NDVI - Normalized Difference Vegetation Index

NDVI is calculated by subtracting the maximum absorption of radiation in the red (R) spectral region from the maximum reflection of radiation in the near infrared (NIR) region. Because green vegetation easily reflects infrared light, it appears brighter. If a plant is subject to stress, it decreases or cease chlorophyll production and will decrease reflects infrared light energy. The vegetation absorbs the red band but reflects the near-infrared band. Natural materials, such as water and carbon content, pigment, and nitrogen, influence reflection and absorption. The NIR band is highly reflected and, hence, detects a healthy reflection of vegetation and dry soil. If the NDVI is close to 0, it may indicate that there is no vegetation cover, however, if it is negative, it may indicate non-vegetation surfaces such as water, asphalt roads, and bare soil. Furthermore, NDVI values are higher in healthy vegetation. But on the other hand, stressed plants might have lower NDVI values (Hashim et al. 2019). NDVI maps that refer to vegetation rate changes based on spectral reflections should be reclassified, the NDVI implementation value range of -1 to 1 is used. Using the NIR and Red bands, the NDVI uses to calculate the balance of energy emitted and obtained by earth objects (Hashim et al. 2019). The NDVI was expressed as follows:

$$\mathrm{NDVI} = \frac{(\mathrm{NIR} - \mathrm{RED})}{(\mathrm{NIR} + \mathrm{RED})} \qquad (1)$$

NIR: Near Infra-Red

According to the methodology used for assessing changes in pasture condition, pasture vegetation surveys are conducted after flowering and germination at the highest yields. To do this, the Landsat 8 image was selected after the end of plant growth, on 18 August 2020.

3.4 Image classification

The goal of the image classification process is to automatically classify all pixel values into land cover types or themes (Thomas & Ralph 2000). One or more spectral or structural characteristic can be used to develop the categorization law. There are two kinds of classification methods: unsupervised and supervised (Shinozuka & Mansouri 2009). The unsupervised classification method is a fully automatic process that does not require any ground truth data. At the image processing step, the defined characteristics of an image are detected in a systematic manner using a suitable algorithm (Shinozuka & Mansouri 2009; Thomas & Ralph 2000). The supervised classification method refers to the process of optically selecting samples within an image and classifying them to pre-selected categories in order to generate statistical measurements that can be associated with a given image (Shinozuka & Mansouri 2009). One of the most widely known supervised classification method is maximum likelihood classification (Shinozuka & Mansouri 2009), that is based on Bayes' theorem and Gaussian distribution. The Bayesian classification algorithm employs two factors to assess the probability. The factors could explain a primary probability for each class or be equivalent to the amount of pixels (Lillesand et al. 2008). When each cell is assigned to one of the classes indicated in the signature file, the tool calculates both the means and covariances of the class signatures. With the assumption that the distribution of a class sample can be described by the mean module and the covariance matrix. The statistical likelihood for every class is computed based on these two characteristics for each cell determining cell membership in the class (ESRI 2021).

3.5 Accuracy assessment

Accuracy assessment is a tool for reviewing classification results by using a describing error or confusion matrix. Each class in the confusion matrix is defined by a comparing of classification results and ground training data (Lillesand et al. 2008). There are several parameters that can be used to determine the accuracy of the classification, such as overall accuracy, user and producer accuracy, and commission (inclusion) and omission (exclusion) errors (Lillesand et al. 2008). The pixels in the training dataset that are correctly classified as land cover run along the massive diagonal of the confusion (error) matrix (Thomas & Ralph 2000). The nondiagonal elements of the matrix are all errors of commission or omission. Nondiagonal column elements correlate to omission errors. Nondiagonal row elements represent commission errors (Thomas & Ralph 2000). The overall accuracy is determined using the total number of correctly classified pixels divided by the total number of reference pixels. To calculate producer accuracy, the correctly classified pixels are divided in each class by the number of training dataset pixels in that category. This parameter indicates how well pixels in the training dataset of the specified cover type are classified. To calculate user accuracies, the number of correctly classified pixels in each class is divided by the total number of pixels classified in that category. This parameter is a measure of commission error and demonstrates the possibility that a pixel categorized into a specific category on the ground truly represents that category (Thomas & Ralph 2000). Table 1 displays the confusion matrix. All the equations are explained in detail below.

Table 1. Error and confusion matrix. (Source: Story & Congalton 1986).

		Ground truth data			Total	Omission	User's accuracy (%)
		A	B	C			
Classified image	a	20	1	2	∑a = 23	0.13	87
	b	4	32	6	∑b = 42	0.24	76
	c	3	7	50	∑c = 60	0.17	83
	Total	∑A=27	∑B=40	∑ =58	N = 125		
	Commission	0.41	0.2	0.14			
	Producer's accuracy (%)	59	80	86			
Overall accuracy = 82%							

$$OA = \frac{aA + bB + cC}{N} = (20 + 32 + 50)/125 \approx 0.82 \quad (2)$$

Equation 2: OA - Overall accuracy, N- total number of ground truth data, bB, aA, and cC – corresponding values

$$OE = \frac{(aB + aC)}{\sum a} = (1 + 2)/23 \approx 0.13 \quad (3)$$

Equation 3: OE - Omission error, ∑a- total number of class pixels in the classified image, aC and aB – values of the class omission,

$$CE = \frac{(bA + cA)}{\sum A} = (4 + 7)/27 \approx 0.41 \quad (4)$$

Equation 4: CE- Comission error, ∑A- total number of pixels in the ground truth data, cA and bA – values of the class commission

$$UA = 1 - OE \quad (5)$$

Equation 5: OE- omission error, UA – user's accuracy

$$PA = 1 - CE \quad (6)$$

Equation 6: CE- commission error, PA – producer's accuracy

4. METHODOLOGY

4.1 Project flow chart

Rangeland degradation mapping consisted of the steps described in the following practical exercise flowchart (Fig. 5). Each step of the analysis is described in detail below.

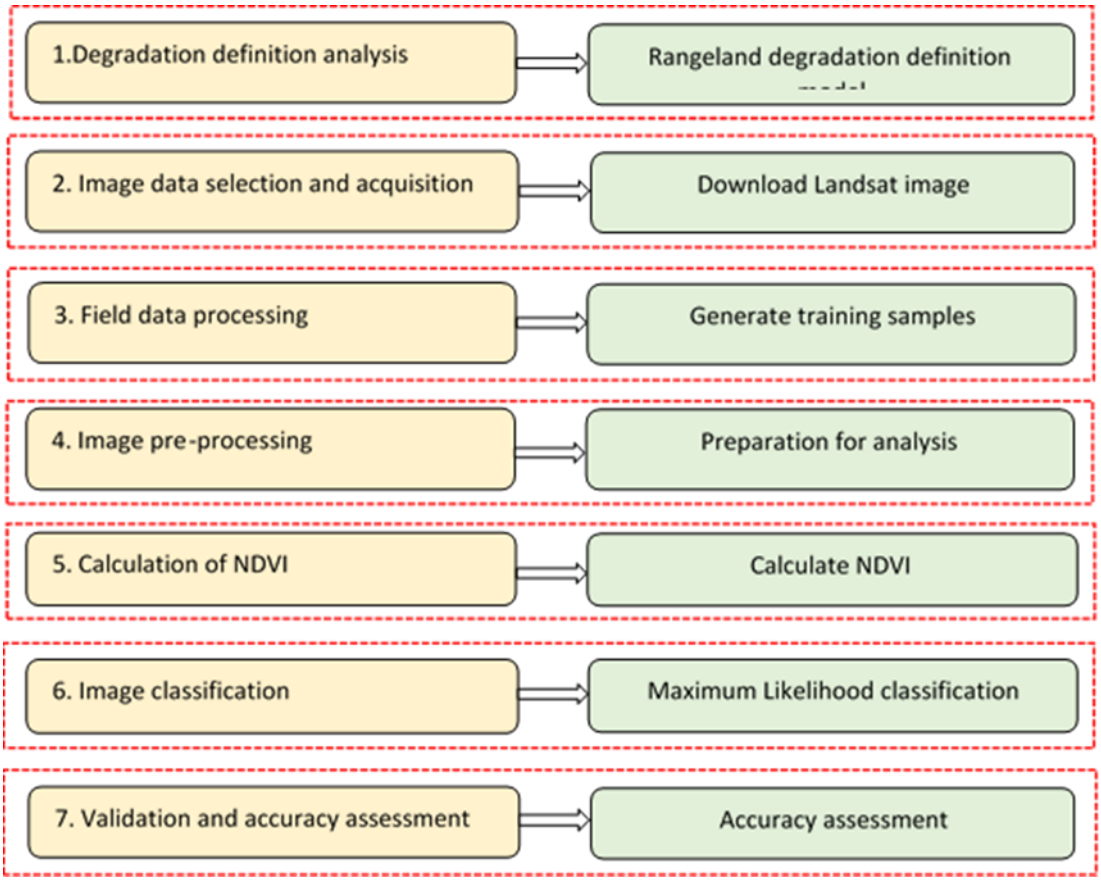

Figure 5. The practical exercise flowchart.

4.2 Degradation definition analysis

Sainbayar et al. (2014) identified the rangeland degradation in Bulgan province, which neighbours the study area and is in same natural zone. Sainbayar et al. (2014) classified rangeland degradation into 4 classes: non-degraded, low, moderate, and high-degraded. In addition, Mongolian rangeland recovery capacity is classified into 4 classes (Densambuu et al. 2018). According to these 2 approaches, in this study the training samples were divided into 4 classes based on NDVI value using ArcGIS Pro 2.6 software. The NDVI values were calculated using Landsat 8 satellite imagery. This is a practical remote sensing approach study done without ground truth measurements with degradation classifications divided into 4 equal intervals of the spectral range based on the calculated values of NDVI, namely non-degraded, low, moderate, and high degraded (Table 2). 150 training samples were generated for each of the 4 classes, making a total of 600 training samples. The high values indicate healthy pasture where degradation has not occurred, and the low values indicate unhealthy pasture or degraded areas. Degradation condition was then classified in descending order from the maximum NDVI values to the low (negative values), starting with healthy or non-degraded followed by slightly degraded, then moderately degraded, and finally severely degraded. Rangeland degradation conditions are described in Table 2.

Table 2. Classification of rangeland degradation.

Degradation condition	NDVI value range	Description
Non degraded	0.39 - 0.64	Healthy rangeland. The condition of the main pasture has not changed.
Low	0.32 - 0.39	Slight changed. Sub-dominant species have changed
Moderate	0.22- 0.32	Moderate changed. Main-dominant species have changed
High	-0.11 - 0.22	Severely degraded. All species have changed, unpalatable plants have predominated

4.3 Image data acquisition

In this study, Landsat-8 data for the 18 August 2020 was utilized. Landsat 8 OLI multispectral image (path 132, row 26) in Landsat Collection 2, Level 1 was selected and downloaded for the purpose of this study from the website http://earthexplorer.usgs.gov. The imagery acquisition time was selected for 18 August 2020 and the whole research area image (almost not affected by clouds) then downloaded (Figure 6). Land cloud cover of this image was 3.29%, deemed suitable for differentiating rangeland degradation classes and mitigating the effects of NDVI changes. As shown in Table 3, spectral characteristics of Landsat 8 satellite data were used in this study.

Table 3. Spectral characteristics of Landsat 8 OLI satellite data.

Bands	Wavelength (micrometre)	Resolution (meter)
Band 1 - Coastal aerosol	0.43 – 0.45	30
Band 2 - Blue	0.45 – 0.51	30
Band 3 - Green	0.53 – 0.59	30
Band 4 - Red	0.64 – 0.67	30
Band 5 - Near Infrared (NIR)	0.85 – 0.88	30
Band 6 - SWIR 1	1.57 – 1.65	30
Band 7 - SWIR 2	2.11 – 2.29	30
Band 8 - Panchromatic	0.50 – 0.68	15
Band 9 - Cirrus	1.36 – 1.38	30
Band 10 - Thermal Infrared (TIRS) 1	10.60 – 11.19	100
Band 11 - Thermal Infrared (TIRS) 2	11.50 – 12.51	100

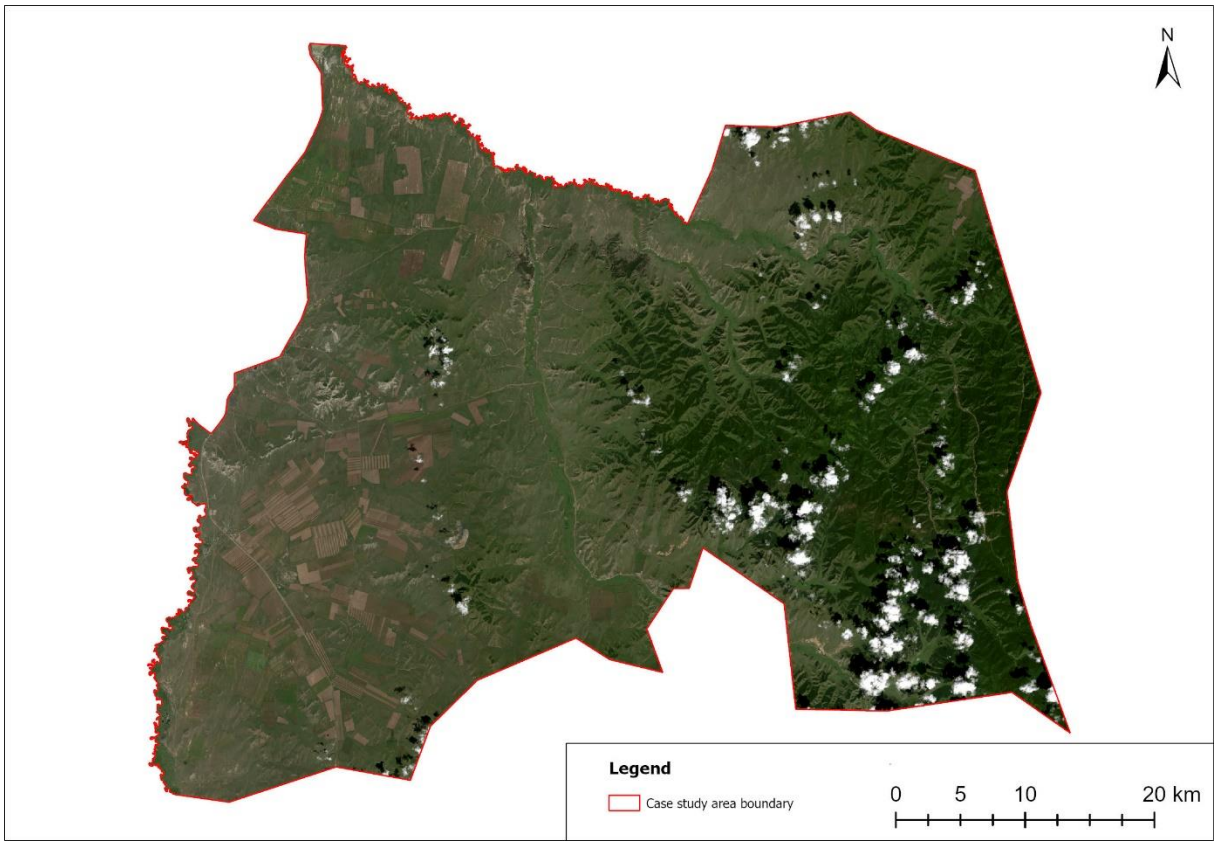

Figure 6. The raw data of case study area in 2020.

4.4 Vector data acquisition

The vector data including research area boundaries, roads, settlement areas, herders' winter-spring camp location points, mines, agricultural areas, forests, rivers, and streams within the selected area was acquired. The data was acquired from the "Darkhan-Uul province unified land territory registration" data, generated by the Land Administration office of Darkhan-Uul province.

4.5 Field data processing

A field measurement is used to conduct rangeland vegetation surveys for ground truthing but due to time restraints, in this study these were not conducted.

In ArcGIS Pro 2.6 software, training samples were generated using the training sample manager tool for classification and accuracy assessment. A total of 800 samples were prepared to calibrate classification and accuracy assessment. The samples were then separated into two groups: the first group was for classification calibration while second for validation and accuracy assessment. In the first group, 75% (n=600) of the total training samples were computed for calibration of image classification using the maximum likelihood classifier in ArcGIS Pro software. The distribution of the training samples for classification is shown in Figure 7.

In this case study, accuracy was calculated in ArcGIS Pro 2.6 software using on second group training samples (n=200) that were randomly selected to ensure accuracy of the results. In the validation section, accuracy assessment was quantitatively evaluated based on 25% of the total

training samples. The distribution of the training samples after accuracy assessment is shown in Figure 8.

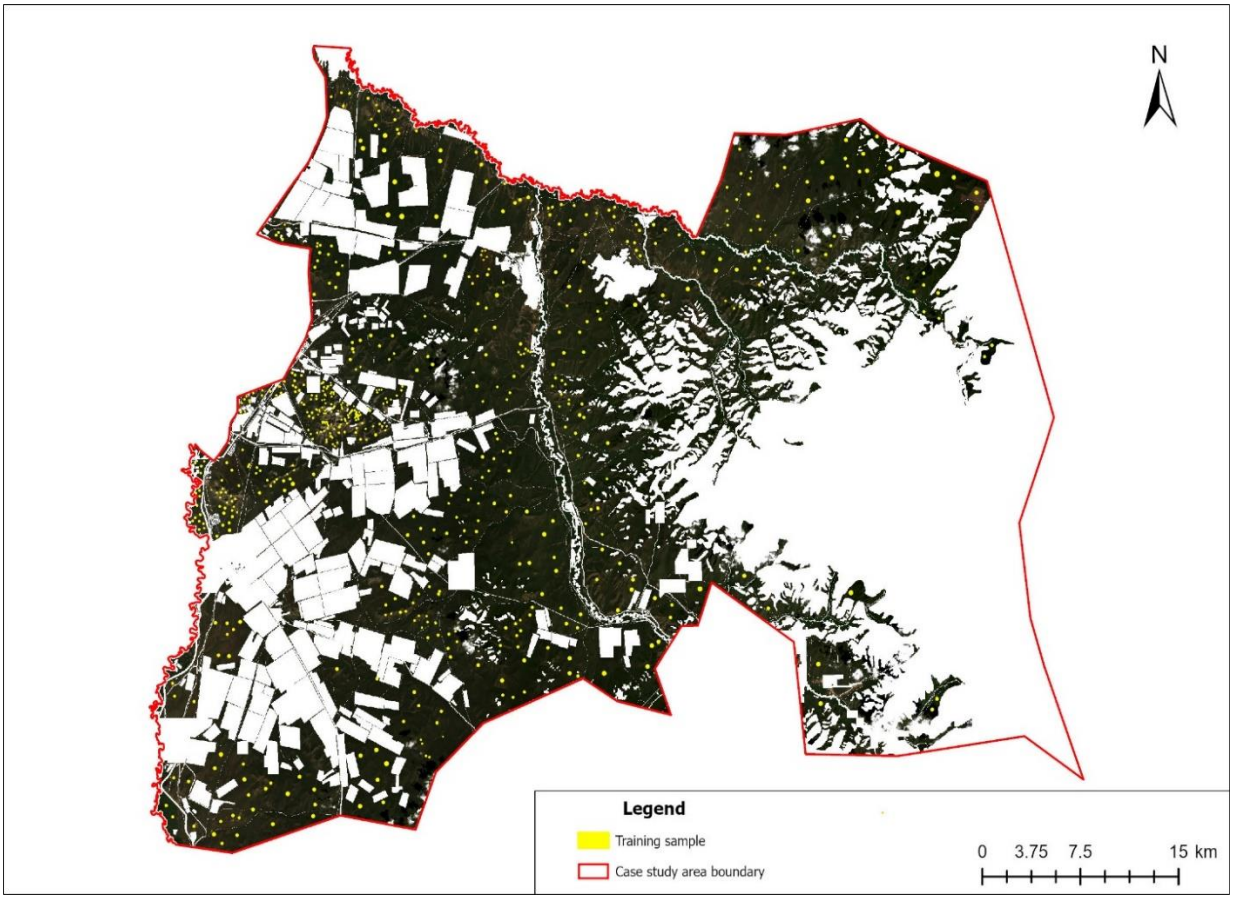

Figure 7. Distribution of training sample data for classification in case study area.

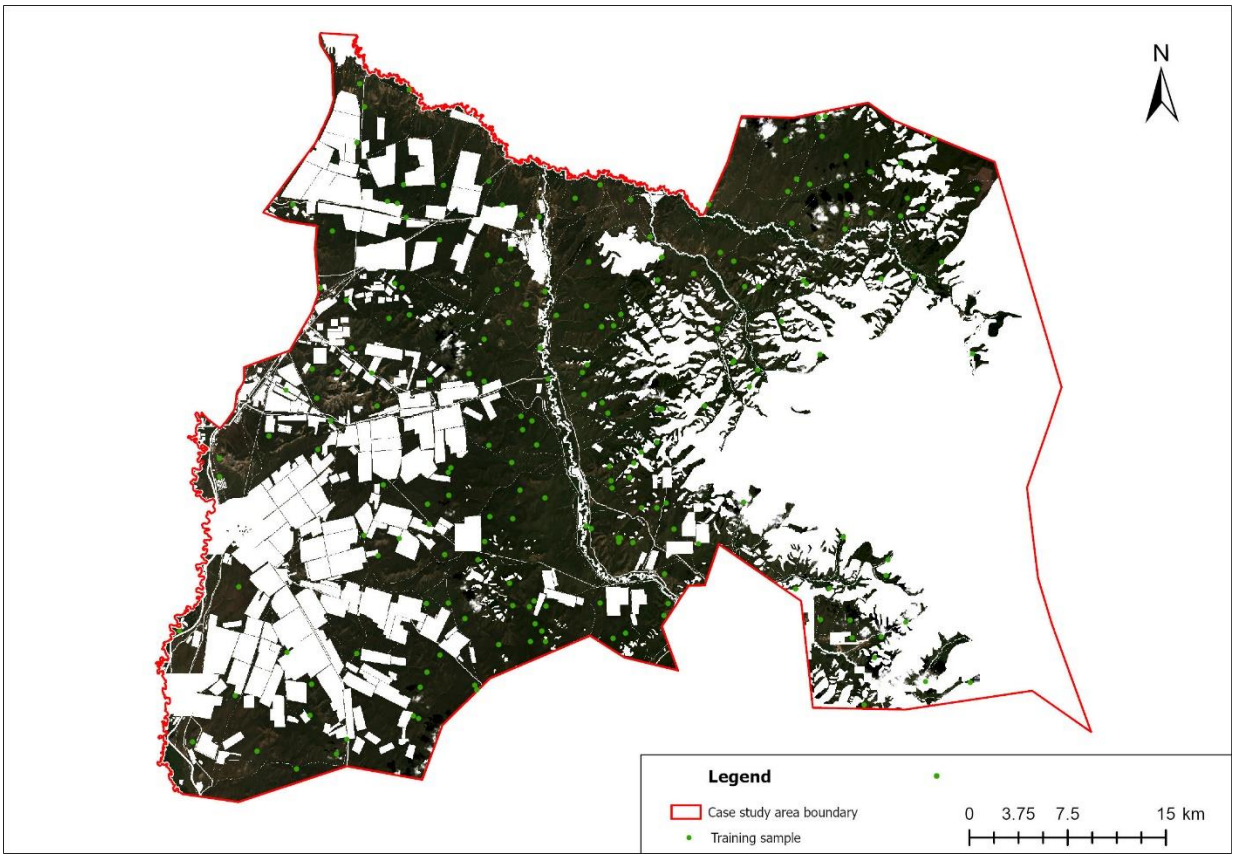

Figure 8. Distribution of training sample data for accuracy assessment in case study area.

4.6 Image pre-processing

The pre-processing step was conducted after selecting and downloading satellite imagery to prepare the image for analysis. First, the satellite image boundary of the research area was cut out. In this case study, only rangeland area was investigated, so other categories of land, such as forest, waterbodies, roads, agricultural areas, mines, and settlement areas were removed from the total area. The boundary cut out was done in ArcMap 10.8.1 software while the removal of the other land class areas was done using the mask tool in the image analysis section using vector data from the basic raw image data. Figure 9 shows a pre-processed Landsat 8 satellite image ready for analysis.

4.7 Calculation of NDVI

The main purpose of this case study is to identify and map degraded rangeland area by NDVI levels and to determine the degree of degradation. In this study, ArcGIS Pro 2.6 software was used to calculate NDVI of the pre-processed image (Figure 9), using Equation 1 to assess rangeland degradation. NDVI calculation was done using Near-Infrared and Red bands in the NDVI tool found in the imagery toolbox which is also found in the Indices tool. The pre-processed image (Fig. 9) file is selected and NDVI parameters calculated with the output file shown in Figure 11.

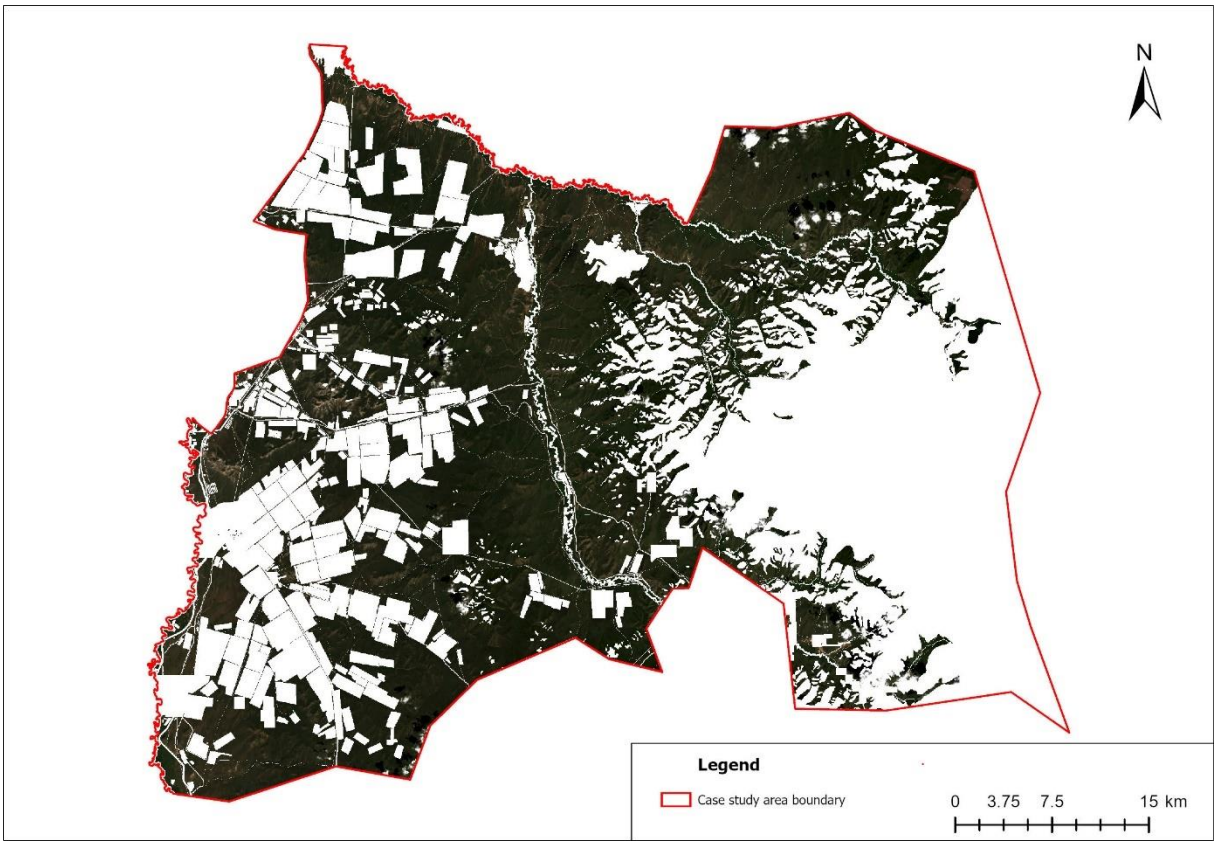

Figure 9. The raw image for NDVI calculation.

4.8 Image classification

The pixel-based maximum likelihood classification was supervised using ArcGIS Pro 2.6 software. Maximum likelihood classification assumes that the statistics for every class in every band are equally distributed and computes the likelihood that a given pixel belongs to a particular class. Before classification, training samples were generated for each 4 classes. The training sample manager tool in ArcGIS Pro 2.6 was utilized for preparation of training samples. The training sample manager tool is the mechanism for managing training samples to create and edit class names or values, save, and evaluate. A training sample was generated based on Landsat-8 satellite data of 18 August 2020 for each 4 classes. A total of 800 samples were prepared to calibrate classification and accuracy assessment, of which 600 training samples were computed for the classification. This means that 75% of the total training sample was used for classification. The 150 points were created manually in each 4 classes using the generate training sample tool in ArcGIS Pro 2.6 software (Table 4).

Table 4. Training samples for classification.

Classification	Training sample	Pixel percent %
Non-degraded	150	23.6
Low	150	39.9
Moderate	150	19.6
High degraded	150	16.9
Total	600	100

Maximum Likelihood Classification was performed by the maximum likelihood classifier tool found in the segmentation and classification menu in the spatial analyst toolbar. Next, the calculated NDVI image (Figure 11) was selected as the input file, and the training sample data selected in the input signature file generated a classified image (Figure 13).

4.9 Validation and accuracy assessment

Accuracy assessment was performed using the classified image (Figure 13) and accuracy assessment points (n=200) performed by accuracy assessment point tool in image analyst tool. This was followed by calculation of the confusion matrix in the Excel software. The overall accuracy including producer's and user's accuracy values were calculated using Equation 2, 5 and 6. Omission and commission errors were calculated using Equation 3 and 4. Each 4 classes were used in the validation section.

5. RESULTS

5.1 NDVI analysis

The maximum NDVI value for this study was 0.64 while the minimum value was -0.10. From the results, the highest NDVI values indicated high and healthy rangeland area, and a negative and low NDVI values indicated low or severely degraded rangeland areas. According to the 4 classes the NDVI values were between 0.64-0.39, 0.39-0.32, 0.32-0.22, 0.22 and -0.10 for non-degraded, low degraded, moderate degraded and high-degraded class, respectively, see Table 5 and Figure 10. Figure 11 shows the distribution of NDVI values in the case study rangeland area.

Table 5. NDVI values.

Classes	Max	Min	Mean	Standard deviation
Non degraded	0.64	0.39	0.52	0.18
Low	0.39	0.32	0.36	0.05
Moderate	0.32	0.22	0.27	0.07
High degraded	0.22	-0.11	0.06	0.23

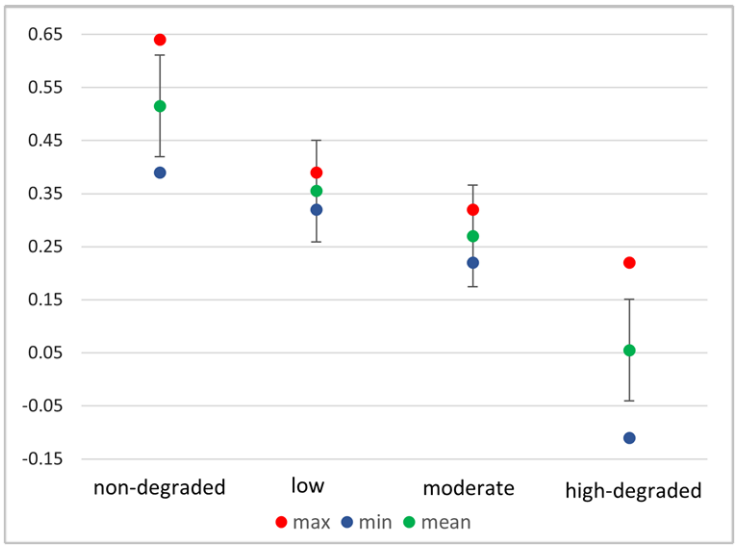

Figure 10. Variation of NDVI value in rangeland degradation classes.

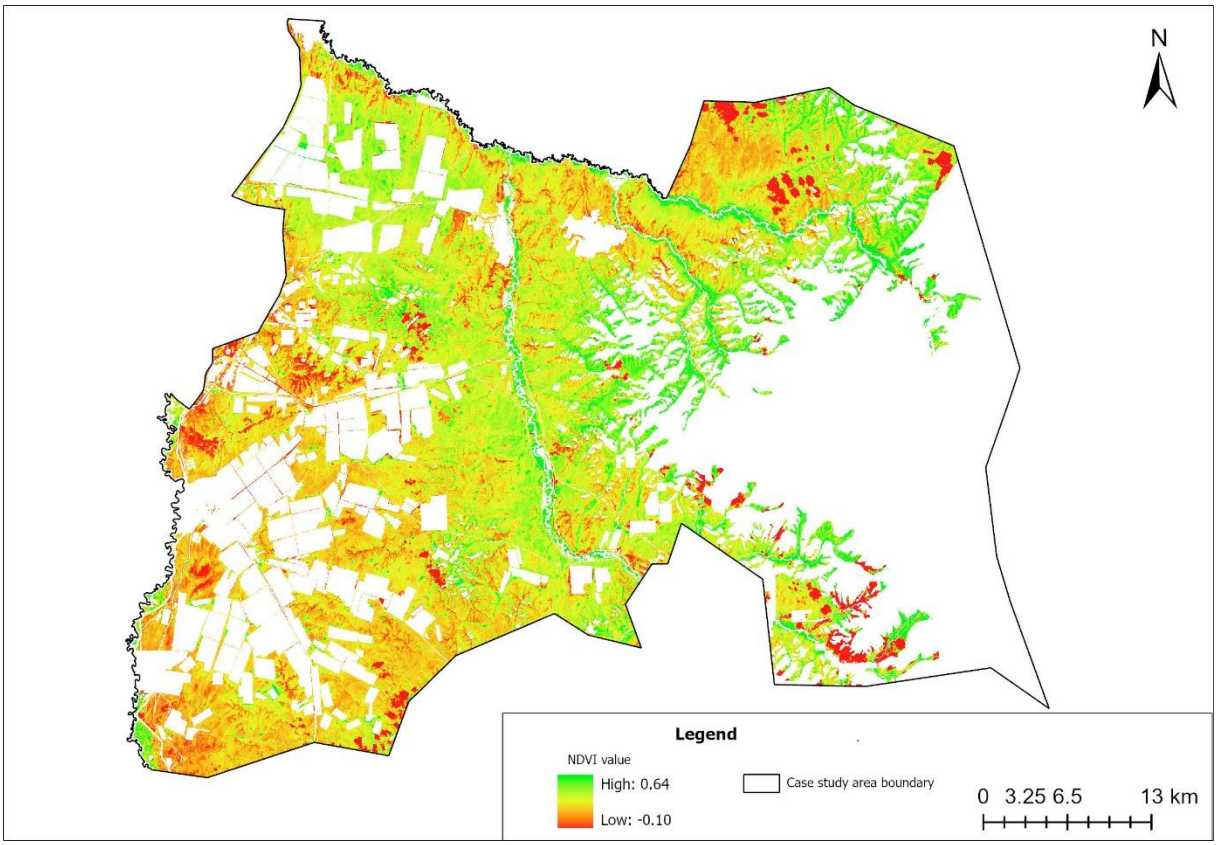

Figure 11. NDVI value of the rangeland in the case study area.

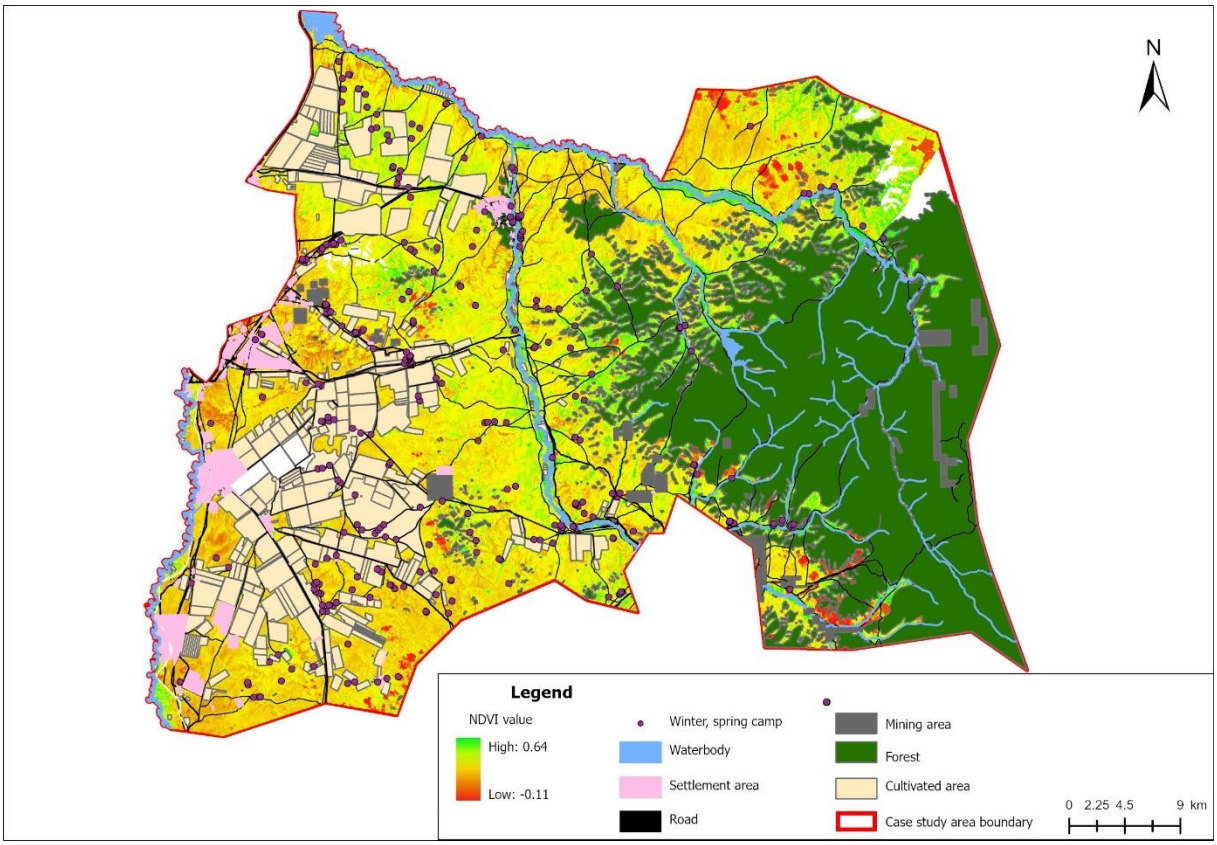

Figure 12. Map showing NDVI values and other land categories in the case study area.

5.2 Image classification

The classified rangeland degradation map of the 18 August 2020 is shown in Figure 13, and the classification results are summarized in Table 6. The results of image classification showed that 35.6% of the total area was in non-degraded, 43.2% in a low degraded, 17.3% in a moderate and 3.9% in a high degraded class in case study area. Basing on the results, the largest proportion of the case study area was in low degraded class followed by non-degraded and the lowest proportion in highly degraded class.

Table 6. Statistical results of rangeland degradation classification.

Rangeland degradation class	Rangeland area		
	sq.km	ha	%
Non degraded	497.29	49729	35.6
Low	603.20	60320	43.2
Moderate	241.92	24192	17.3
High degraded	54.36	5436	3.9
Total	1396.77	139677	100

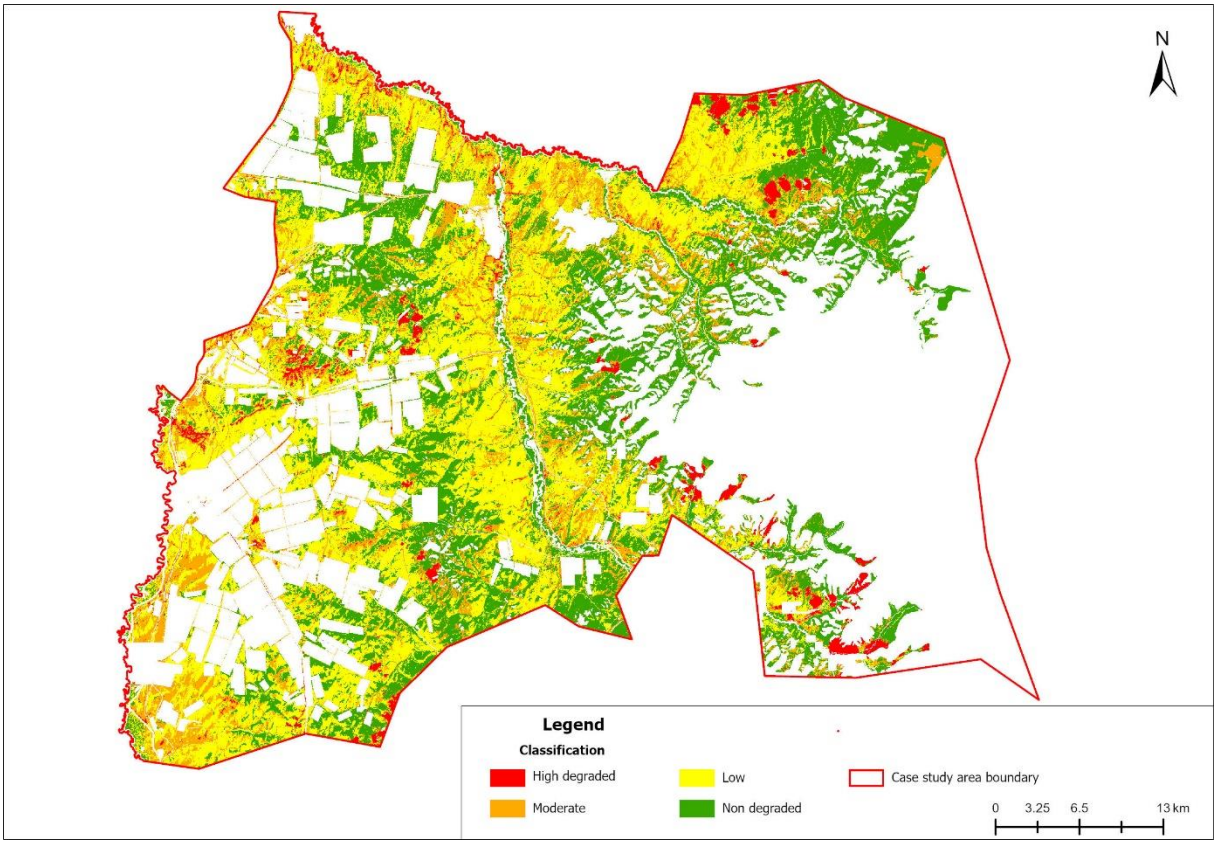

Figure 13. Map of rangeland degradation classification.

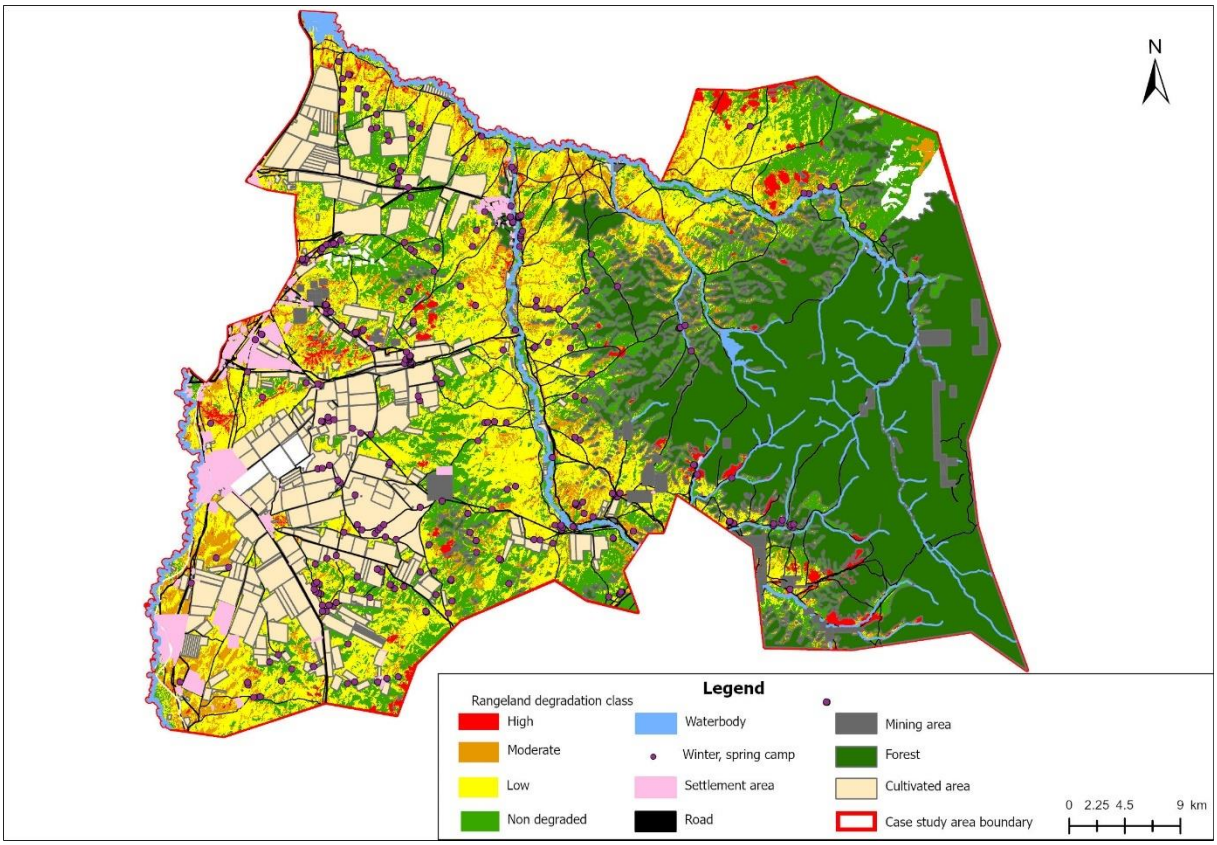

Figure 14. Map of rangeland degradation classification and other land categories.

5.3 Accuracy assessment

The achieved overall accuracy of the supervised Maximum Likelihood classification of the case study area on 18 August 2020 was 69%. The results of the classification accuracy assessment are shown in Table 7.

According to the findings, the highest producer accuracy was associated with the non-degraded class. For this class the producer's accuracy was 74%. The producer's accuracy fell into the low degraded class with 70%, moderate class 68%, and high-degraded class 25%. The value of the user's accuracy was observed to be 80% in non-degraded class, 79% in low degraded class, 50% in moderate class, and 11% in high-degraded class.

Commission and omission errors per class were calculated for specific rangeland degradation classes. The identified commission errors in the maximum likelihood analyses were found at a rate of 75% in the high-degraded class, 32% in the moderate degraded class, 30% in the low degraded class, and 26% in the non-degraded class. Omission errors from the classes high degraded, moderate, low, and non-degraded class were 89%, 50%, 21%, and 20%, respectively.

Table 7. Confusion matrix obtained with Maximum Likelihood Classifier for the 2020 rangeland degradation classification in the Khongor soum of Darkhan Uul province.

Classes		Derived from satellite image data				Total	Omission error	User's accuracy
		Non-degraded	Low	Moderate	High-degraded			
Training sample data	Non-degraded	49	9	3	0	61	0.20	80%
	Low	10	67	6	2	85	0.21	79%
	Moderate	4	16	21	1	42	0.50	50%
	High-degraded	3	4	1	1	9	0.89	11%
Total		66	96	31	4	**200**		
Commission error		0.26	0.30	0.32	0.75			
Producer's accuracy		74%	70%	68%	25%			
Overall accuracy: 69%								

6. DISCUSSION

6.1 Definition of degradation

In this study NDVI values were important for analysing rangeland classification and accuracy assessment of classification. To start with, non-degraded (0.39-0.60), low degraded (0.32-0.39), moderate degraded (0.22-0.32) and high-degraded (-0.11-0.22) classes helped to classify non-degraded areas (35.6%), low degraded areas (43.2%), moderately degraded areas (17.3%) and, high-degraded (3.9%). However, to date, no study has generated NDVI values from an area in Mongolia of similar agroecological zone, land uses and soils. Therefore, the classifications used in this study could be a basis for a more extensive study that incorporates ground truthing. One study by Badrakh (2019), that also used only NDVI calculation, was conducted in a neighbouring area under the same agroecological zone. According to that study, without ground truthing, the NDVI value range was 0.4-0.7 and categorised as 0.4-0.5 for degraded and >0.5 for non-degraded areas. The NDVI values in this study differed from the Badrakh (2019) study values, since the NDVI value for non-degraded areas was >0.39. This difference could probably be due to the difference in the data time line. The Badrakh study was made in 2019, and it is likely that precipitation and air temperature could have been different from this study period. On the other hand in the Badrakh (2019) study area, mining is the main land use which could also probably contribute to the vegetation degradation, while in this study the area consisted of alternating cropland where grazing is the main land use and cropping is in August. Also when this study was compared to Bayaraa (2019) whose study included ground truth data from Bornuur soum, Tuv province, in the same agroecological zone but with grazing as the main land use, the NDVI value was –0.39–0.91 with high overlap compared to this study. Therefore, it may be advantageous to classify degradation based on NDVI values without external or human intervention.

6.2 Field data

Due to the lack of ground truth data survey, it was not reliable to classify rangeland degradation. Badrakh (2021) conducted a study on land use and land cover changes without ground truth

data survey, which identified changes in land use and land cover changes in three time periods. Perhaps this study could have been better at detecting changes in rangeland degradation if data sets from more than one year had been used. Furthermore, longitudinal data sets should be complimented with establishing several control points for each class to monitor the study area (ground truthing). If ground truth data survey is conducted with appropriate equipment, experienced specialists and, availability of logistics, reliability is ensured. However, it is time consuming and costly to process the aggregate these two methods. In this study, however, due to time constraint and because a main goal was to acquire skills in GIS and remote sensing, it had to be done quickly and at low cost.

6.3 NDVI – Normalized Difference Vegetation Index

The results showed that the area in Khongor soum is a rangeland with alternating cropland and grazing as the main land uses. During the study period, the NDVI values ranged between -0.10 and 0.64 with an average of 0.34. Sainbayar et al. (2014) on the other hand identified an NDVI average of 0.56 for rangeland in the northern part of Mongolia, close to the study area for this study, for the period 2000-2014, while employing the same method but with ground truthing. This study had a lower NDVI mean value than the study of Sainbayar et al. (2014). Although the classification used in this study is like the above-mentioned research, it is not possible to compare the values of the two studies because Sainbayar et al. (2014) performed ground truthing which could account for the differences in the two studies.

The results of this case study demonstrate that the low and moderate classes were difficult to differentiate due to spectral overlapping of NDVI values. The NDVI value chart (Figure 10) shows that the spectral range of the high-degraded class overlapped slightly with the moderate class, though it could still be significantly distinguished. Between the low and moderate classes, spectral values highly overlapped. As such, spectral overlaps between the classes could not be significantly distinguished.

According to meteorological data during the study period, the precipitation was lower than the average summer precipitation and the air temperature 1.9 degrees higher than the average summer temperature (IRIMHE 2021), which may also have affected the NDVI values (Hao et al. 2011). However, it is not possible to make a detailed comparison, because the data for this study did not account for more than one year.

6.4 Classification

The expectation of the study was that the high-degraded and moderate degraded areas would be larger than the low and non-degraded classes' areas. Instead, the findings revealed that low and non-degraded classes' area were larger than the other classes. The reason for this might be related to the spectral overlapping or image processing errors. The 150 training samples were obtained for each 4 classes for the classification because the training samples were assumed to be the same number in each class while varying the pixels number in each class and may have influenced the classification. For instance, the percentage of training samples in the low degraded class was the highest for pixel size (39.9%) while the low degraded rangeland was the largest area 43.2% from classification, out of the total rangeland study area. However, the training samples with the smallest pixel number was also the smallest area out of total rangeland study area. Training samples that are insufficient in number, are not representative of the features of interest, or have multimode distributions frequently result in poor classification results (Bayaraa 2019).

6.5 Accuracy assessment

The overall accuracy achieved from the supervised classification was moderate at 69%. However, it is believed to have been more likely to occur because the number of points used for accuracy assessment were relatively small (200 points) compared to the size of the study area (139,677 ha). Another reason could be that the number of points used for the accuracy assessment was unbalanced for each class.

6.6 General evaluation of study findings

This study demonstrated that remote sensing is a time-efficient method of evaluating large areas in a short period of time. However, studies identifying rangeland degradation through remote sensing and moderate resolution images have limitations because of the complication of the rangeland systems.

The results of this case study demonstrated that the classes were difficult to differentiate due to overlapping in the training sample generation. As a pilot study with the objective of acquiring GIS and remote sensing skills for further training the exercise has, however, served its purpose.

The high-degraded class had a low user's accuracy, but high producer's accuracy, which may result in overall low classification accuracy. Additionally, the validation points were too small in high-degraded class. The main reason for the high commission and omission errors in high-degraded class was due to the small and unbalanced sample size.

To achieve good results in this study, 200 points were planned for validation and classification accuracy assessment. However, these have demonstrated that they were not enough number of points in each class for accuracy in classification. Therefore, increasing the number of training samples and keeping the balanced number of points in each class would improve the accuracy of classification in future studies.

7. CONCLUSIONS

The overall goal of this study was to assess the practical use of remote sensing to identify rangeland degradation in Khongor soum of Darkhan-Uul province in Mongolia. This study illustrated that remote sensing can be a relatively quick tool for assessing rangeland vegetation cover changes over large areas in short period of time. Therefore, it was a good learning experience but there are several areas of interest that would require further analysis and an improvement in the methodology for better analysis. A future study could be more interesting if it was based on ground truth data to identify changes in a rangeland over a period of several years for the implementation of substantial management measures.

In future studies, I recommended an increase in the number of points, taking an equal number of points for each class, and to generate the training samples based on the compatible pixel number to improve the quality of the classification.

ACKNOWLEDGEMENTS

I would like to express my gratitude to the GRÓ LRT programme for the great opportunity given to me to study in Iceland and the support rendered to me during my stay in Iceland. My special thanks specifically go to the programme director - Sjöfn Vilhelmsdóttir, deputy programme director - Berglind Orradóttir, office manager - Halldóra Traustadóttir, project manager - Brita Berglund and Steinunn Garðarsdóttir.

I would also like to extend my special thanks to my supervisor Atli Guðjónsson and to the project coordinator Berglind Orradottir, for their productive comments in my research project work. With their generous support and help, I improved my knowledge and learned a lot. Also, I would also like to thank all the lecturers who shared their knowledge and experiences.

Many thanks to my GRÓ LRT 2021 fellows and my friends for the mutual support we had during the last six months when we were together and developed an unforgettable friendship.

LITERATURE CITED

Altanbagana M, Suvdantsetseg B, Chuluun T, Nominbolor H (2015) Эмзэг байдлын үнэлгээнд тулгуурлан ногоон хөгжлийн бодлогыг хэрэгжүүлэх нь Ховд аймгийн жишээгээр. Pages 195–200. Монгол орны бэлчээрийн нөхөн сэргэх чадамжийг бэхжүүлэх нь: сэдэвт салбар хөрвөсөн эрдэм шинжилгээний олон улсын хурал. Цогт принт, Улаанбаатар

Archer RS, Erik MA, Katharine IP, Susanne S, Robert RS, Steven RW (2017) Woody plant encroachment: Causes and Consequences. Pages 25–72. In: David DB (ed.) Rangelands Systems: Processes, Management and Challenges.

Badrakh M (2019) Шарын голын нүүрсний ил уурхай орчмын газар ашиглалт, газрын бүрхэвчийн өөрчлөлтийн судалгаа. Шинжлэх ухааны Академи, Геологийн хүрээлэн. Улаанбаатар

Batima P, Natsagdorj L, Gombluudev P, Erdenetsetseg B (2005) Observed Climate Change in Mongolia. Ulaanbaatar

Batjargal Z, Batjargal H, Tegshjargal B, Solongo B, Saruul D (2015) Дэлхийн Уур Амьсгалын Өөрчлөлтийг Сааруулахад Монгол Улсын Хувь Нэмэр тайлан. Улаанбаатар

Bayaraa B (2019) Assessment of rangeland condition using remote sensing technology: A case study of forest steppe zone in Mongolia. United Nations University Land Restoration Training Programme [final project]
https://www.grocentre.is/static/gro/publication/721/document/bayaraa2019.pdf

Booth T, Tueller P (2003) Rangeland monitoring using remote sensing. Arid land research and management. 17:455–467

Boschetti M, Bocchi S, Brivio P (2007) Assessment of pasture production in the Italian Alps using spectrometric and remote sensing information. Agriculture, Ecosystems and Environment 118:267–272

Cao R, Chen J, Shen M, Tang Y (2015) An improved logistic method for detecting spring vegetation phenology in grasslands from MODIS EVI time-series Data. Agricultural and Forest Meteorology 200:9–20

Colombo R (2012) Assessment of Mediterranean pasture condition using MODIS normalized difference vegetation index time series. Journal of Applied Remote Sensing 6:063530

Densambuu B, Indree T, Battur A, Sainnemeh S (2018) (a) Монгол орны зонхилох бэлчээрийн төлөв байдал, өөрчлөлтийн загварууд. ГЗГГЗЗГ, Швейцарийн Хөгжлийн агентлаг, Монголын Бэлчээр Ашиглагчдын Нэгдсэн Холбоо, Ус Цаг уур, Орчны Судалгаа Мэдээллийн Хүрээлэн, ШУА Ерөнхий болон Сорилын Биологийн Хүрээлэн. Улаанбаатар

Densambuu B, Sainnemeh S, Brandon B, Ulambayar B (2018) (b) National Report on the Rangeland Health of Mongolia: Second Assessment. Green Gold-Animal Health project, SDC; Mongolian National Federation of PUGs. Ulaanbaatar

Eddy IMS, Gergel SE, Coops NC, Henebry GM, Levine J, Zerriffi H, et al. (2017) Integrating remote sensing and local ecological knowledge to monitor rangeland dynamics. Ecological Indicators 82:106–116

ESRI (2021) Tool Reference: Geoprocessing Tools-How Maximum Likelihood Classification works. https://pro.arcgis.com/en/pro-app/latest/tool-reference/spatial-analyst/how-maximum-likelihood-classification-works.htm/ (accessed 15 August 2021)

FAO (Food and Agriculture Organization) (2019) Trees, Forests and Land Use in Drylands: The First Global Assessment-Full report. FAO Forestry Paper No. 184. Rome. Page FAO Forestry Paper Rome www.fao.org/%0Awww.fao.org/publications

Fenetahun Y, Xu X, Wang Y (2018) Assessment of Range Land Degradation, Major Causes, Impacts, and Alternative Rehabilitation Techniques in Yabello Rangelands Southern Ethiopia. Review paper:1–19

Fontana F, Rixen C, Jonas T, Aberegg G, Wunderle S (2008) Alpine Grassland Phenology as seen in AVHRR, vegetation, and MODIS NDVI Time Series - A Comparison with In-situ Measurements. Sensors 8:2833–2853

GEF (2014) Land degradation. https://www.thegef.org/topics/land-degradation (accessed 24 May 2021)

Harris RB (2010) Rangeland Degradation on the Qinghai-Tibetan plateau: A Review of the Evidence of Its Magnitude and Causes. Journal of Arid Environments 74:1–12

Hao F, Zhang X, Quyang W, Andrew K, Skidmore A, Toxopeus G (2011) Vegetation NDVI Linked to Temperature and Precipitation in the Upper Catchments of Yellow River. Environment Model Assess 17: 389-398

Hashim H, Abd Latif Z, Adnan NA (2019) Urban vegetation classification with NDVI threshold value method with very high resolution (VHR) Pleiades Imagery. International Archives of the Photogrammetry, Remote Sensing and Spatial Information Sciences - ISPRS Archives 42:237–240

Hilker T, Natsagdorj E, Waring R, Lyapustin A, Wang Y (2014) Satellite observed widespread decline in Mongolian grasslands largely due to overgrazing. Global Change Biology 20:418–428

Holechek J, Pieper R, Herbel C (2011) Range Management Principles and Practices. Prentice Hall, New Jersey

ILRI, IUCN, FAO, WWF, UNEP, ILC (2021) Rangelands Atlas. ILRI, Nairobi, Kenya

Jigjsuren O, Baival B, Naynaa H, Jargalsaihan A, Dash H, Bud A et.al. (2015) Уур Амьсгалын Өөрчлөлтийн Нөлөөллийг Малчдын Ажиглалтаар Үнэлж, Цаг Уурын Болон Зайнаас Тандан Судлалын Мэдээтэй Харьцуулах нь. Улаанбаатар

Karneili A, Bayarjargal Y, Bayasgalan M, Mandakh B, Dugarjav C, Burgheimer J, et al. (2013) Do Vegetation Indices Provide a Reliable Indication of Vegetation Degradation? A case Study in the Mongolian Pastures. International journal of Remote sensing 34:6243–6262

Lillesand T, Kiefer R, Chipman J (2008) Digital Image Interpretation and Analysis. Pages 482–623. Remote Sensing and Image Interpretation. John Wiley & Sons. InC, New Jersey

Mariano D, Santos CAC, Wardlow B, Anderson M, Schiltmeyer A, Tadesse T, et al. (2018) Use of Remote Sensing Indicators to Assess Effects of Drought and Human-Induced Land Degradation on Ecosystem Health in North-eastern Brazil. Remote Sensing of Environment 213:129–143

Matongera TN, Mutanga O, Sibanda M, Odindi J (2021) Estimating and Monitoring Land Surface Phenology in Rangelands: A review of Progress and Challenges. Remote Sensing 13:109-117

Ministry of Environment and Green Development (2018) Монгол орны байгаль орчин. Ulaanbaatar

Ministry of Nature Environment and Green Development (2014) Монгол орны уур амьсгалын өөрчлөлтийн үнэлгээний хоёрдугаар илтгэл. Ulaanbaatar

Misra G, Cawkwell F, Wingler A (2020) Status of phenological research using sentinel-2 data: A review. Remote Sensing 12:10–14

IRIMHE (Mongolian Information and Research Institute of Meteorological Hydrological and Environment) (2021) Overview of weather conditions in Darkhan-Uul province http://tsag-agaar.gov.mn/(accessed 15 August 2021)

Narmandakh A (2009) Land Use Planning of Darkhan-Uul province. Ulaanbaatar

NSO (National Statistical Office of Mongolia) (2020) https://www.1212.mn/ (accessed 18 August 2021)

NSO (National Statistical Office of Mongolia) (2019) https://www.1212.mn/ (accessed 18 August 2021)

Nguyen LH, Joshi DR, Clay DE, Henebry GM (2020) Characterizing land cover/land use from multiple years of Landsat and MODIS time series: A novel approach using land surface phenology modelling and random forest classifier. Remote Sensing of Environment 238:111017

Petros M (2005) Morphological Filtering for Image Enhancement and Feature Detection. Pages 135–156. Handbook for Image and Video Processing. National Technical University of Athens. Athens

Pinto CT, Jing X, Leigh L (2020) Evaluation analysis of landsat level-1 and level-2 data products using in situ measurements. Remote Sensing 12:1–30

Sainbayar D, Sainbuyan B, Altantuya D, Narangerel B, Danzanchadav G (2014) Байгалийн болон хүний хүчин зүйлийн нөлөөллийг тооцоолон газрын доройтол, цөлжилтийг үнэлэх нь. ШУА-ын Газарзүй-Геоэкологийн Хүрээлэн, Зурагзүй Газарзүйн Мэдээллийн Системийн Салбар. Улаанбаатар

Shankar N, Ramaseri C, Jon BC, Kimberly AC (2020) 2020 Joint Agency Commercial Imagery Evaluation- Remote Sensing Satellite Compendium. Virginia

Shen M, Piao S, Dorji T, Liu Q, Cong N, Chen X, et al.. (2015) Plant phenological responses to climate change on the Tibetan Plateau: Research status and challenges. National Science Review 2:454–467

Shinozuka M, Mansouri B (2009) Synthetic Aperture Radar and Remote Sensing Technologies for Structural Health Monitoring of Civil Infrastrucrture Systems. Pages 113–151. Structural Health Monitoring of Civil Infrastructure systems. Woodhead Publishing Series in Civil and Structural Engineering

Story M, Congalton RG (1986) Remote Sensing Brief Accuracy Assessment: A User's Perspective. Photogrammetric Engineering and Remote Sensing 52:397–399

Svoray T, Perevolotsky A, Atkinson P (2013) Ecological Sustainability in Rangelands: The Contribution of Remote Sensing. International Journal of Remote Sensing 34:6216–6242

Thomas LM, Ralph KW (2000) Remote Sensing and Image Interpretation. Page: 12-46 (M. Clifford and P. Marian, Eds.) Danver, USA

Tomaszewska MA, Nguyen LH, Henebry GM (2020) Land Surface Phenology in the Highland Pastures of Montane Central Asia: Interactions with Snow Cover Seasonality and Terrain Characteristics. Remote Sensing of Environment 240:111675

Tong X, Tian F, Brandt M, Liu Y, Zhang W, Fensholt R (2019) Trends of Land Surface Phenology Derived from Passive Microwave and Optical Remote Sensing Systems and Associated Drivers Across the Dry Tropics 1992–2012. Remote Sensing of Environment 232:111307

Ünal E, Mermer A, Yildiz H (2014) Assessment of rangeland vegetation condition from time series NDVI data. Journal of Field Crops Central Research Institute 23:14–21

United Nations (2019) World Population Prospects 2019. Department of Economic and Social Affairs. New York. http://www.ncbi.nlm.nih.gov/pubmed/12283219

USEPA (United States Environmental Protection Agency) (2017) Agricultural Pasture, Rangeland, and Grazing. New York. https://www.epa.gov/agriculture/agricultural-pasture-rangeland-and-grazing (accessed 18 August 2021)

USGS (2020) Mapping, Remote Sensing and Geospatial Data.
https://www.arcgis.com/home/webmap/ (accessed 18 August 2021)

USGS (2021) My Map. https://www.arcgis.com/home/webmap/viewer.html?useExisting=1 (accessed 18 August 2021)

Vanderpost C, Ringrose S, Matheson W, J Arntzen (2011) Satellite Based Long Term Assessment of Rangeland Condition in Semi-arid Areas: An example from Botswana. Journal of Arid Environments 75:383–389

Vrieling A, Meroni M, Darvishzadeh R, Skidmore AK, Wang T, Zurita-Milla R, et al.. (2018) Vegetation Phenology from Sentinel-2 and field cameras for a Dutch barrier island. Remote Sensing of Environment 215:517–529

Zhou W, Yang H, Huang L, Chen C, Lin X, Hu Z at. al. (2017) Grassland Degradation Remote Sensing Monitoring and Driving Factors Quantitative Assessment in China from 1982 to 2010. Ecological Indicators 83:303–313

APPENDIX

Project: Mapping rangeland degradation: A theoretical and practical exercise in the forest steppe zone, Mongolia

Date : 18/08/2021
Author: Erdenechimeg Avidsuren
Input:

Data	Khongor soum imagery data (Mongolia, Darkhan-Uul province)
Sensor	Landsat 8 (# path: 132 # row : 26)
Data captured	18/08/2020
Corresponding field data acquisition	July 2021 (http://earthexplorer.usgs.gov.)
Product type	Collection 2, Level 1
Land cloud cover	3.29 %
Resolution	30m

Output:

		Khongor soum imagery data
Pre-processing	Radiometric Correction	**X**
	Atmospheric Correction	**X**
	Masking	✓
Image classification		✓
Error assessment		✓

Software: ArcGIS 10.8.1 and ArcGIS Pro 2.6

Date	Step	Input and outputs of processing	Processing steps and notes
Creating a single raster dataset from multiple bands			
Date: 18/08/2021	**Processing step:** Creating a single raster dataset **Software:** ArcGIS Pro **Remark:** Landsat 8 OLI has 11 single raster datasets	**Input**: L8C 11 single raster datasets **Output:** L8C_composite	1. Open ArcGIS Pro and load raw image data. 2. Open the Geoprocessing tool – Data Management toolbox 3. Raster toolset- Raster processing toolset - Composite Bands 4. Proceed every band in the input raster section respectively. 5. Select an appropriate output file name and folder to save the composite image. 6. Select Run.
Preparing image for analysis			
Date: 18/08/2021	**Processing step:** Making a mask raster dataset to use **Software:** ArcGIS Pro **Remark:**	**Input**: L8C_composite **Output:** L8C_composite_mask	1. Open Add Data - L8C_composite 2. Open Add Data – Soum_boundary (shape file) 3. Arc Toolbox-Spatial Analyst Tools - Extraction – Extract by mask 4. Proceed raster dataset in the input raster section. 5. Select a raster or feature mask data. (In this case soum boundary shape file was used) 6. Select an appropriate output file name and folder to save. 7. Select Run.
Date: 19/08/2021	**Processing step:** Masking out other land categories area from total soum area **Software:** ArcMap 10.8.1 **Remark:** In this study only rangeland area is used	**Input**: L8C_composite_mask **Output:** Research_area_image	1. Open Add Data - L8C_composite_mask 2. Open Add Data – mining_area (shape file) 3. Forest, waterbody, road, agricultural area, mining, and settlement area were cut out in separately for each of these 6 categories. This operation was repeated 6 times. 4. Windows menu – Image analysis 5. In Image analysis window select basic raster dataset (L8C_composite_mask) 6. Select mask tool
Making a classification			
Date: 19/08/2021	**Processing step:** Creating classification schema **Software:** ArcGIS Pro **Remark:**	**Input**: Research_area_image **Output:** Training_samples	1. Open Add Data - Research_area_image 2. Imagery menu – Classification tool 3. Open Training samples manager tool 4. Start creating a new classification schema. Select Create new schema tool. This is a new classification schema for study 5. Move the mouse to the new schema and right-click to create a new category. Create 4 classes. In this window put the name, colour, and value of the category.

			6. Select Ok. 7. In this way, each of the 4 categories is repeated and done. 8. Select an appropriate file name and location to store the training samples
Date: 19/08/2021	**Processing step:** Creating training samples **Software:** ArcGIS Pro **Remark:**	**Input**: Research_area_image **Output:** Training_samples_class	1. Open Add Data - Research_area_image 2. Imagery menu – Classification tool 3. Open Training samples manager tool 4. Select the class to create the training samples, select drawing tool (polygon, circle, rectangle) and create the training samples. 5. In this way, 150 training samples created for each 4 classes. Total 600 samples 6. Select save. An appropriate file name and location to store the training samples.
Calculating NDVI			
Date: 20/08/2021	**Processing step:** Calculating NDVI **Software:** ArcGIS Pro **Remark:**	**Input**: Research_area_image **Output:** Research_area_NDVI	1. Open Add Data - Research_area_image 2. Imagery menu – Indices tool 3. Open NDVI tool 4. Select a raster data and select an appropriate output file name and folder to save. Select Run.
Creating classification and validating			
Date: 20/08/2021	**Processing step:** Creating classification **Software:** ArcGIS Pro **Remark:**	**Input**: Research_area_NDVI **Output:** Research_area_classified	1. Open Add Data - Research_area_NDVI 2. Select Analysis menu – Tools 3. Spatial Analyst Tools – Segmentation and classification menu – train Maximum Likelihood Classifier 4. In Geoprocessing section select input raster, select Input training sample, select an appropriate output classifier definition file name and folder to save. 5. Select Run.
Date: 21/08/2021	**Processing step:** Validating classification **Software:** ArcGIS Pro **Remark:**	**Input**: Research_area_classified **Output:** Acc_ass_points	1. Open Add Data - Research_area_classified 2. Select Analysis menu – Tools 3. Spatial Analyst Tools – Segmentation and classification menu 4. Create accuracy assessment points – select input raster as Research_area_classified 5. Select as output accuracy assessment points an appropriate file name and location to store 6. Number of random points are 200 7. Select Run
Date: 21/08/2021	**Processing step:** Validating classification	**Input**: Research_area_classified	1. Open Add Data - Research_area_image

	Software: ArcGIS Pro **Remark:**	**Output:** Accuracy_ass	2. Select Analysis menu – Tools 3. Spatial Analyst Tools – Segmentation and classification menu 4. Update accuracy assessment points – select input raster as Research_area_classified 5. Select input accuracy assessment points as Acc_ass_points 6. Select as output accuracy assessment points an appropriate file name and location to store 7. Select Run